J. Opt. A: Pure Appl. Opt. **10** (2008) 104007 (5pp) doi:10.1088/1464-4258/10/10/104007

The speckle photo-electromotive force on a vanadium-doped CdTe crystal

T O Santos[1], J C Launay[2], S G Odoulov[3] and J Frejlich[1]

[1] Laboratório de Óptica—IFGW-UNICAMP, Campinas-SP, Brazil
[2] ICMCB, CNRS, Université Bordeaux 1, France
[3] Institute of Physics, National Academy of Sciences of Ukraine, Kiev, Ukraine

Received 7 March 2008, accepted for publication 22 May 2008
Published 27 August 2008
Online at stacks.iop.org/JOptA/10/104007

Abstract
The photo-electromotive force (photo-emf) generated by a vibrating laser speckle pattern at 1064 nm in the bulk of a photorefractive vanadium-doped CdTe crystal is used to evaluate the sample's response time and the vibration amplitude of the speckle pattern. We measured the first harmonic temporal term of the photocurrent, under different conditions, as a function of the vibration amplitude, vibration frequency, and irradiance, in order to verify some features of the theoretical model for large vibration amplitude speckle photo-emf. The most interesting feature is the presence, for sufficiently fast vibrations, of a maximum in this first harmonic term at a fixed vibration amplitude-to-speckle size ratio whose position should depend only on the dark conductivity to photoconductivity ratio. The presence of such a maximum is experimentally confirmed and opens the way for rather simple calibration of the setup in practical applications. We also demonstrate the application of this photo-emf signal to evaluate the material response time of the CdTe:V crystal.

Keywords: speckle, photorefractive, vibrations, CdTe, photoconductor, photo-emf

1. Introduction

A photo-electromotive force (photo-emf) is induced in a photoconductive (not necessarily photorefractive) material when a vibrating spatial distribution of light intensity is projected onto it [1–5]. The distribution of light may be an interference [3, 6, 7] or a speckle [5, 8] pattern of light. The vibration of this pattern produces an alternating current in the photoconductor. This effect results from the movement of photoexcited space charge carriers in the conduction band (or valence band for holes) in the presence of a stationary space charge field produced by the pattern of light. The latter field results from the progressive accumulation of photoexcited charge carriers in deep recombination centers in the darker regions of the material [1, 2]. Since the first experimental results involving photo-emf in photorefractive materials were published [9], many interesting applications have been developed based on this effect, among which we can point out the measurement of mechanical vibrations [5, 8] and the detection of phase-modulated optical signals [1, 10]. In 2001, Stepanov published a detailed work about the photo-emf effect [11], that consists of the theoretical description, experimental data in different photoconductive and photorefractive materials, and applications. Many photorefractive and photoconductive materials have already been successfully used in speckle photo-emf experiments, including BTO [3, 5], GaAs [8, 2], and CdTe [12, 13]. In 2004, Mosquera and Frejlich [5] showed that the photocurrent signal exhibits a maximum for a certain vibration amplitude Δ (normalized over the size of the speckle) that may be used as a reference to calibrate the setup. Experimental results carried out on $Bi_{12}TiO_{20}$ (BTO) [5] and CdTe:V [14] crystals did roughly confirm the presence of such a maximum.

In this paper we report and analyze some experimental results of speckle photo-emf in CdTe:V for transverse vibration amplitude measurement and also show the application of this technique for material characterization.

Speckle photo-emf techniques are particularly interesting because they require a very simple experimental setup: a direct laser beam shining on the vibrating target to be measured, an independent sensor head holding the photorefractive crystal with or without some electronics inside, and a current measurement mode lock-in amplifier. On the other hand, the theoretical model is much more complicated than that for interference-based experiments. The speckle

photo-emf is peculiar in the sense that, in contrast to the interference-based technique, it directly measures the transversal vibration component. Photorefractive CdTe:V crystals are interesting materials for photo-emf because of their relatively low dark (deleterious) conductivity and high (necessary) photoconductivity at 1064 nm wavelength light. A good-quality laser beam at 1064 nm is easily obtained at relatively high CW power and low cost from Nd–YAG lasers. CdTe, however, exhibits a rather fast response time so, as will be shown latter on, it is better suited for ultrasonic rather than audio or lower frequency vibrations. The very simple setup involved in these experiments allows us to easily change the operating laser wavelength as well as the photorefractive crystal sensor to fit any specific application, either for vibration or material response measurements.

2. Theory

When a rough surface is illuminated by coherent (laser) light, it generates a random granular (with average radius R) pattern of light intensity, called a speckle. The oscillatory movement of this speckle on a photoconductive material induces an alternative photocurrent i that depends on the transverse oscillation amplitude Δ, among other parameters. This amplitude and the resulting photocurrent are not linearly related, and the latter exhibits harmonic terms of the vibration (angular) frequency Ω. The first harmonic (i^{Ω}) photocurrent term is particularly interesting for the measurement of Δ, and was already theoretically shown (see [14]) to be described as

$$i^{\Omega} \propto f(I, \delta, R_{\mathrm{d}}), \tag{1}$$

where $f(I, \delta, R_{\mathrm{d}})$ represents a function of the irradiance I, $\delta \equiv 2\Delta/R$, and $R_{\mathrm{d}} \equiv \sigma_{\mathrm{d}}/\sigma_{\mathrm{ph}}$, where R is the speckle radius and σ_{d} and σ_{ph} the dark conductivity and the photoconductivity, respectively. For vibration frequencies Ω much higher than the photorefractive crystal response time τ_{SC} fulfilling the condition

$$\Omega\tau_{\mathrm{SC}} \gg 1, \tag{2}$$

the first harmonic term in equation (1) does not depend on τ_{SC}. Otherwise, equation (1) should be modified to take into account the material response time [1]

$$i^{\Omega} = f(I, \delta, R_{\mathrm{d}}) \frac{\tau_{\mathrm{SC}}\Omega}{\sqrt{1 + (\tau_{\mathrm{SC}}\Omega)^2}}, \tag{3}$$

which is true at least for small values of δ. The parameter τ_{SC} is proportional to the Maxwell (or dielectric) relaxation time τ_{M} [3, 15]

$$\tau_{\mathrm{SC}} \propto \tau_{\mathrm{M}} = \epsilon\varepsilon_0/\sigma, \tag{4}$$

$$\sigma = \sigma_{\mathrm{ph}} + \sigma_{\mathrm{d}} \qquad \sigma_{\mathrm{ph}} \propto I, \tag{5}$$

where ϵ is the dielectric constant, ε_0 the permittivity of vacuum, and the other parameters were already defined above. While τ_{M} depends only on the material, τ_{SC} also depends on geometric parameters such as, in this case, the speckle radius R.

The theoretical model for large amplitude speckle photo-emf signals has already been described in detail elsewhere [14],

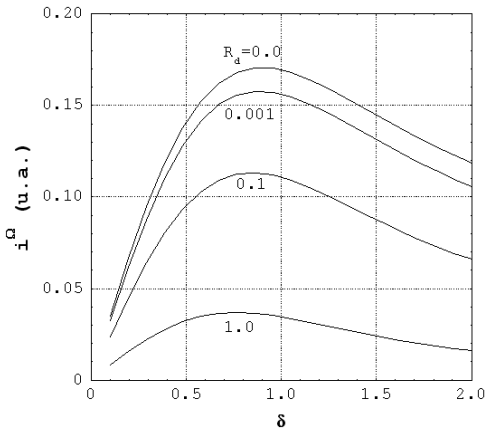

Figure 1. Theoretical plot of i^{Ω} versus δ for different values of $R_{\mathrm{d}} = 0.0, 0.01, 0.1$ and 1.0. Note the position of the maximum being slightly shifted to lower values as R_{d} increases.

where it was theoretically demonstrated that its first harmonic term, represented by equation (1), should exhibit a maximum at a characteristic value of δ that depends only on R_{d}, as far as the condition in equation (2) is fulfilled. The computed results are represented in figure 1, where i^{Ω} is plotted as a function of δ for different values of R_{d} varying from 0.0 to 1.0, with the corresponding position of the maximum varying from 0.90 to 0.76.

It has already been shown [14], and will be reported here too, that if the condition in equation (2) is not fulfilled, the maximum of i^{Ω} is shifted along higher values of δ and may even not show up at all. In this case one may take advantage of the τ_{SC} dependence of i^{Ω} for computing the material response time, as will be demonstrated below.

3. Experimental details

A speckle photo-emf experiment was carried out using a sample of a vanadium-doped cadmium telluride (CdTe:V) crystal labeled BR4ZM1/b. The light propagates along the $d = 2.6$ mm sample's thickness. The electrodes are painted with conductive silver glue on the lateral faces (transverse to the light propagation), separated by the interelectrode distance $\ell = 4.2$ mm. The height of the crystal is $h = 9.39$ mm. The experimental setup is shown schematically in figure 2. A CW laser beam with $\lambda = 1064$ nm and linear polarization parallel to the target vibration direction (in its turn parallel to the ℓ crystal dimension) is shining on the vibrating target. The latter is a thin transparent ground glass plate attached to the cone of a commercial loudspeaker. The light transmitted through the ground glass plate is collected by a photographic objective (F-number $= 2$) and focused onto the crystal volume. The distance from the target to the input lens plane was $L_{\mathrm{tl}} = 238$ mm and the lens focus was 50 mm, which resulted in a 0.21 lens magnification of the target displacement projected onto the CdTe:V crystal. The amplitude and (angular) frequency Ω of the loudspeaker are controlled by a signal generator. The vibration amplitude of the target was measured using laser Doppler velocimetry [16, 17]. The photocurrent was collected

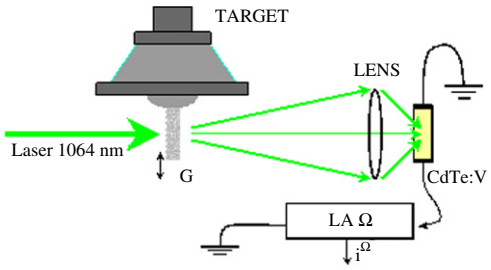

Figure 2. Schematic representation of the setup. The target is a diffusing glass plate **G** attached to the cone of a commercial loudspeaker; the photocurrent is collected by lateral electrodes on the photorefractive crystal and fed to a lock-in amplifier tuned to Ω.
(This figure is in colour only in the electronic version)

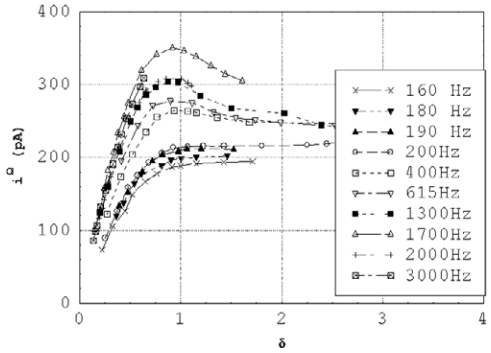

Figure 3. First harmonic photocurrent component i^{Ω} as a function of the normalized vibration amplitude δ for different frequencies in the range 160 Hz–3000 Hz and a fixed irradiance $I(0) = 3.78$ mW cm^{-2}.

from the sample volume by lateral electrodes (transverse configuration), and the first harmonic i^{Ω} was measured using a lock-in amplifier. For practical reasons the irradiance $I \propto V_{\mathrm{PD}}$ (with 1 V corresponding to approximately 90 μW cm^{-2} at this 1064 nm wavelength) was measured at the output rear face of the CdTe:V crystal using a photodetector placed just behind and very close to the sample. The intensity absorption coefficient of this sample at $\lambda = 1064$ nm was experimentally found to be $\alpha = 320$ m^{-1}, and its refractive index at this wavelength is 2.74 [18]. From these data it is possible to compute the irradiance at the input plane inside the sample $I(0) \approx 3I$ from the value of the measured irradiance I at the output.

4. Results and discussions

The current i^{Ω} is measured as a function of the normalized parameter δ (figures 3, and 4) for different Ω and a constant irradiance $I(0) = 3.8$ mW cm^{-2} estimated at the input plane inside the sample from the irradiance $I = 1.26$ mW cm^{-2} behind the crystal. It should be noted that the dependence of i^{Ω} versus δ is not the same for $\Omega \gg 1/\tau_{\mathrm{SC}}$ and for $\Omega \ll 1/\tau_{\mathrm{SC}}$. In the former case the current i^{Ω} features a quite pronounced maximum at $\delta \approx 0.9$ (see, for example, $\Omega/2\pi = 1700$ Hz in figure 3) and its position is not affected by Ω within a wide

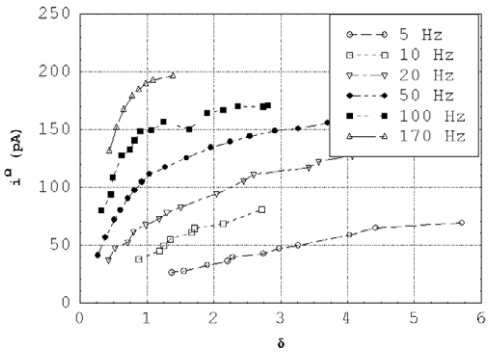

Figure 4. First harmonic photocurrent component i^{Ω} as a function of the normalized vibration amplitude δ for different frequencies in the range 5 Hz–170 Hz and a fixed irradiance $I(0) = 3.78$ mW cm^{-2}.

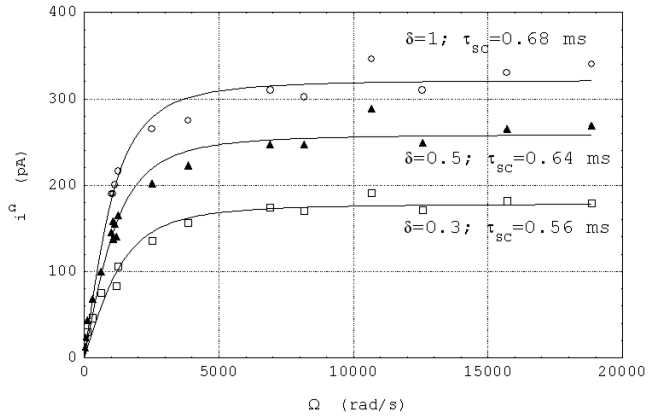

Figure 5. First harmonic photocurrent component i^{Ω} data as a function of frequency for $\delta = 1$, 0.5 and 0.3, with $I(0) = 3.78$ mW cm^{-2}. The continuous lines are the best fitting with equation (3), leading to the corresponding different values for τ_{SC} indicated in the figure.

range. For low Ω, however, the maximum does not show up and i^{Ω} increases monotonically with δ as shown, for example, for $\Omega = 5$ Hz in figure 4.

From the data in figures 3 and 4 it is possible to deduce the frequency response at a fixed irradiance. To do so we plot the values of i^{Ω} measured at a fixed δ as a function of Ω, as shown in figure 5 for three different values for δ and a fixed $I(0) = 3.8$ mW cm^{-2}. This figure shows qualitatively the expected result: a sharp increase from $\Omega = 0$ on and a saturation at larger values for Ω. The solid lines are the best fit of equation (3), and from this fit we obtained $\tau_{\mathrm{SC}} = 0.68$, 0.64 and 0.56 ms for the corresponding $\delta = 1$, 0.5 and 0.3. These different values for τ_{SC} are certainly due to the fact that equation (3) is verified for low amplitude vibrations only, so the lower the value of δ the better the computed τ_{SC} value. Accordingly we chose the curve with $\delta = 0.3$ in figure 5 as the most representative one for extracting the response time τ_{SC} at this irradiance. We repeated this experiment for different irradiances but always with the same $\delta = 0.3$, and plotted the corresponding τ_{SC} as a function of the irradiance in figure 6, where we see that with the dark decay taken into account the relations in equations (4) and (5) are roughly verified.

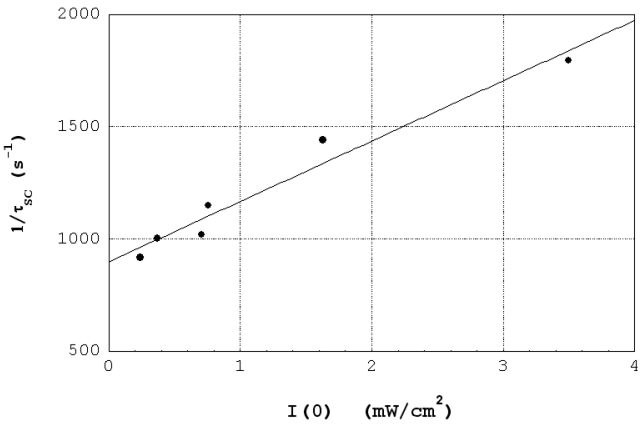

Figure 6. Inverse response time as a function of the irradiance at a fixed $\delta = 0.3$.

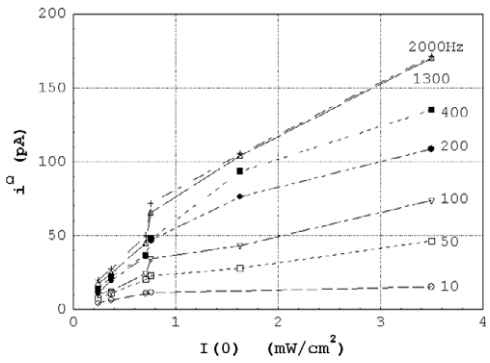

Figure 7. First harmonic photocurrent component i^{Ω} as a function of the irradiance for different frequencies, always for $\delta = 0.3$.

The intensity dependence of i^{Ω} for different Ω and fixed δ in figure 7 shows interesting features: for rather low Ω and irradiances I larger than a threshold value the i^{Ω} is independent of I. For much larger Ω, however, i^{Ω} increases steadily with I and, in the limit, becomes independent of Ω. These results are in qualitative agreement with the model of a photocurrent generated by charge carriers moving on a space–charge field: the measured current is high and tends to saturation for larger vibration frequencies for which the space charge can be considered to be immobile, not able to follow fast variations of the speckle pattern, as in figure 5. For frequencies in this range the largest current roughly corresponds to the vibration amplitude equal to the speckle size, as shown in figure 3. At low frequencies, however, $\Omega < 1/\tau_{SC}$, the space charge pattern is able to follow slow spatial variations of the speckle pattern and the current is therefore nearly vanishing. The residual current nevertheless increases linearly with the increasing vibration amplitude. This can be explained by the fact that the speed of the speckle grain motion for a given frequency increases linearly with the amplitude of the vibration. Therefore the effective misalignment (displacement) between the space–charge and speckle patterns appears to be proportional to the vibration amplitude δ even beyond $\delta \approx 1$.

The results in this paper show a trade-off of practical interest as far as vibration measurement is concerned: for low frequencies the response is almost linear with δ and almost independent of I, which is convenient for amplitude measurement, but the signal is much lower than at higher frequencies. For higher frequencies the response is much higher, shows a maximum at a roughly fixed reduced amplitude value that could be used for calibrating the setup, and, in the $\Omega\tau_{SC} \gg 1$ limit, it is independent of frequency. In this condition the i^{Ω} signal is very convenient for vibration amplitude measurement with the drawback of being very dependent on the irradiance.

The reader should be aware that the speckle size radius R in this paper was computed to be the size of the diffraction limited spot (Airy function) produced by the focusing lens in the setup. If the lens is not perfect (diffraction limited) the actual speckle size may be larger than the theoretically computed one in this paper.

We did not consider here the effect of the bulk material light absorption, which for this sample and wavelength produces a roughly 0.4-fold reduction in irradiance through its 2.6 mm thickness. Such a variation, however, is not very relevant here because the useful speckle pattern is limited to a region in the crystal of depth a few micrometers (comparable to the focal depth of the focusing lens, that is roughly computed from $\lambda(F\text{-number})^2 \approx 4\ \mu$m [19]) where the irradiance can be considered to be practically constant. On the other hand, while seeking to maximize the signal in the experiments we are automatically adjusting the speckle close to the input crystal plane where the irradiance is higher, and the signal too.

5. Conclusions

This paper reports speckle photo-emf experiments using a vanadium-doped photorefractive CdTe crystal (CdTe:V) to explore the possibilities and limitations of this technique for the measurement of transverse vibrations and for material characterization. We have experimentally confirmed the theoretically predicted presence of a maximum in the first harmonic photocurrent signal. However, as CdTe is a rather fast material, only the higher frequency vibrations fulfill the theoretical $\Omega\tau_{SC} \gg 1$ condition for producing a frequency independent signal showing a maximum at a fixed reduced amplitude δ value with special interest for vibration amplitude applications. Lower frequency experiments, however, do not exhibit such a maximum, and are very sensitive to the material response time. Therefore experiments in this condition are particularly suited for material characterization, and the dark conductivity to photoconductivity ratio for this sample was characterized in this way to illustrate the procedure. From the shape of first harmonic photo-emf signal as a function of the vibration amplitude for the lower frequencies it becomes evident that material response time effect on the photo-emf signal as formulated in equation (3) is only an approximation, which may be considered only for low amplitudes. The experimental setup is a very simple one, and the illumination laser wavelength as well as the detection photorefractive crystal can be easily substituted to fit different applications.

Acknowledgments

The authors are grateful to the Conselho Nacional de Desenvolvimento Científico e Tecnológico (CNPq) and Fundação de Amparo à Pesquisa do Estado de São Paulo (FAPESP) for financial support.

References

[1] Stepanov S, Sokolov I, Trofimov G, Vlad V, Popa D and Apostol I 1990 Measuring vibration amplitudes in the picometer range using moving light gratings in photoconductive GaAs:Cr *Opt. Lett.* **15** 1239–41

[2] Korneev N A and Stepanov S 1993 Non-steady-state photoelectromotive force in semiconductor crystals with high light absorption *J. Appl. Phys.* **74** 2736–41

[3] Sokolov I A and Stepanov S I 1993 Non-steady-state photoelectromotive force in crystals with long photocarrier lifetimes *J. Opt. Soc. Am.* B **10** 1483–8

[4] Stepanov S I 1994 Applications of photorefractive crystals *Rep. Prog. Phys.* **57** 39–116

[5] Mosquera L and Frejlich J 2004 Self-calibrating speckle photo-electromotive-force for large vibration amplitude measurement *J. Opt. A: Pure Appl. Opt.* **6** 1001–4

[6] Petrov M P, Sokolov I A, Stepanov S I and Trofimov G S 1990 Non-steady-state photo-electromotive-force induced by dynamic gratings in partially compensated photoconductors *J. Appl. Phys.* **68** 2216–25

[7] Bryushinin M, Kulikov V and Sokolov I 2002 Nonresonant enhancement of the nonstationary holographic currents in photoconductive crystals *Phys. Rev.* B **65** 2452041–6

[8] Korneev N A and Stepanov S I 1991 Measurement of small lateral vibrations of speckle patterns using a non-steady-state photo-emf in GaAs:Cr *J. Mod. Opt.* **38** 2153–8

[9] Trofimov G S and Stepanov S I 1986 Time-dependent holographic currents in photorefractive crystals *Sov. Phys.—Solid State* **28** 1559–62

[10] Stepanov S I 1994 Sensitivity of non-steady-state photoelectromotive force-based adaptive photodetectors and characterization techniques *Appl. Opt.* **32** 915–20

[11] Stepanov S I 2001 Photo-electromotive-force effect in semiconductors *Semiconductor Devices* (*Handbook of Advanced Electronic and Photonic Materials and Devices* vol 2) ed H S Nalwa (New York: Academic) chapter 6, pp 205–72

[12] Mansurova S, Seres Rodríguez I, Stepanov S and Trivedi S 1999 Non-steady-state photo-EMF effect in semiinsulating CdTe associated with fundamental optical absorption *CLEO* 509–10

[13] Stepanov S I, Rodríguez P, Mansurova S, Arroyo M L, Trivedi S and Wang C C 2007 Wavelength dependence of the photo-electromotive-force effect in CdTe:V crystal with bipolar photoconductivity *Opt. Mater.* **29** 623–30

[14] dos Santos T, Launay J and Frejlich J 2008 Photo-electromotive-force from large amplitude transverse speckle pattern light vibration *J. Appl. Phys.* **103** 1131041–6

[15] Frejlich J 2006 *Photorefractive Materials: Fundamental Concepts, Holographic Recording, and Materials Characterization* (New York: Wiley–Interscience)

[16] Belansky R and Wanser K 1993 Laser Doppler velocimetry using a bulk optic Michelson interferometer: a student laboratory experiment *Am. J. Phys.* **61** 1014–9

[17] Freschi A A, Kamshilin A A and Frejlich J 1992 Doppler velocimetry for photodetector frequency response measurement *Opt. Commun.* **90** 193–6

[18] Marfaing Y 1999 State of the art and prospects of photorefractive CdTe *J. Cryst. Growth* **197** 707–17

[19] Born M and Wolf E 1975 *Principles of Optics* 5th edn (Oxford: Pergamon)